BIOCHEMISTRY
including biophysical chemistry & molecular biology

Accelerated Publication

pubs.acs.org/biochemistry

Molecular Mechanism of Photoactivation and Structural Location of the Cyanobacterial Orange Carotenoid Protein

Hao Zhang,[†,‡] Haijun Liu,[‡,§] Dariusz M. Niedzwiedzki,[‡,§] Mindy Prado,[‡,§] Jing Jiang,[‡,∥] Michael L. Gross,[†] and Robert E. Blankenship*[,†,‡,§]

[†]Department of Chemistry, [‡]Photosynthetic Antenna Research Center (PARC), [§]Department of Biology, and [∥]Department of Energy, Environmental and Chemical Engineering, Washington University in St. Louis, One Brookings Drive, St. Louis, Missouri 63130, United States

Supporting Information

ABSTRACT: The orange carotenoid protein (OCP) plays a photoprotective role in cyanobacterial photosynthesis similar to that of nonphotochemical quenching in higher plants. Under high-light conditions, the OCP binds to the phycobilisome (PBS) and reduces the extent of transfer of energy to the photosystems. The protective cycle starts from a light-induced activation of the OCP. Detailed information about the molecular mechanism of this process as well as the subsequent recruitment of the active OCP to the phycobilisome are not known. We report here our investigation on the OCP photoactivation from the cyanobacterium *Synechocystis* sp. PCC 6803 by using a combination of native electrospray mass spectrometry (MS) and protein cross-linking. We demonstrate that native MS can capture the OCP with its intact pigment and further reveal that the OCP undergoes a dimer-to-monomer transition upon light illumination. The reversion of the activated form of the OCP to the inactive, dark form was also observed by using native MS. Furthermore, *in vitro* reconstitution of the OCP and PBS allowed us to perform protein chemical cross-linking experiments. Liquid chromatography−MS/MS analysis identified cross-linking species between the OCP and the PBS core components. Our result indicates that the N-terminal domain of the OCP is closely involved in the association with a site formed by two allophycocyanin trimers in the basal cylinders of the phycobilisome core. This report improves our understanding of the activation mechanism of the OCP and the structural binding site of the OCP during the cyanobacterial nonphotochemical quenching process.

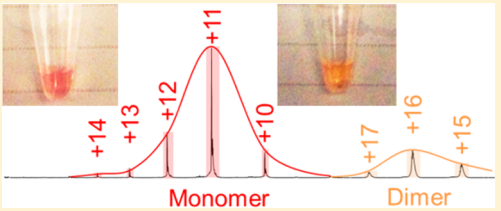

Cyanobacteria primarily collect light via the phycobilisome (PBS), a megadalton extramembrane antenna pigment−protein complex containing covalently bound bilin pigments.[1] In addition to the pigmented phycobiliproteins, pigment-free linker proteins play important roles in assembly and in maintaining a functional core-and-rod structure.[2] Energy collected by the PBS rapidly migrates from rods to the core and subsequently is transferred to a membrane-embedded reaction center of Photosystem II (PSII) or Photosystem I (PSI). Under saturating light conditions, most cyanobacteria induce a photoprotective mechanism in which excess absorbed energy is dissipated as heat in a process called non-photochemical quenching (NPQ), which decreases the amount of energy arriving at the PSII and PSI reaction centers.[3] Two proteins, the orange carotenoid protein (OCP) and the fluorescence recovery protein (FRP), are known to be involved in photoprotection and restoring the full capacity of the light harvesting function, although the mechanistic details of this process have not been elucidated.[4,5]

The OCP is a 35 kDa water-soluble protein. Krogmann's group[6,7] first reported the isolation and characterization of the OCP before its photoprotective function had been established. Crystal structures of the OCP have been determined from *Arthrospira maxima*[8] and *Synechocystis* sp. PCC 6803.[5] The OCP contains a single molecule of 3′-hydroxyechinenone (3′-hECN), a carotenoid having 11 conjugated carbon−carbon double bonds. It is the first photosensory protein discovered with carotenoid as the pigment.[4] Both N- and C-terminal domains bind the pigment (3′-hECN) such that it is almost buried in the crystal structure of the OCP.[8] The OCP and photoprotective function in cyanobacteria were linked together by Kirilovsky's group.[9,10] In darkness or nonsaturated light conditions, the OCP is orange (OCP^o). The photoactivation of the OCP can be triggered by blue-green light, which converts the OCP^o into a red form (OCP^r). The active OCP^r is metastable and quickly converts back to the inactive form (OCP^o) in the dark. Previous spectroscopic studies demonstrated that both the OCP and pigment (3′-hECN) undergo dramatic conformational changes upon blue-green light illumination,[10−13] indicative of the intimate interactions of the pigment and the apo-OCP. Genetic results demonstrated that in the absence of the OCP, the fluorescence of PBS cannot be quenched in cyanobacteria. In the presence of excess OCP, faster fluorescence quenching of PBS is observed.[14] *In vitro* reconstitution studies indicated that only the OCP^r is competent to bind PBS and triggers fluorescence quenching.[15]

Received: November 15, 2013
Revised: December 18, 2013
Published: December 21, 2013

The FRP, a 13 kDa protein on an operon with the OCP in most cyanobacterial species,[16] can accelerate the release of the OCP from PBS and thus recover the PBS fluorescence in the dark.[16]

Even though structural models of the OCP have been proposed,[8,17] there are still questions about how the transition between the OCP^o and the OCP^r takes place and whether there are any changes in the oligomeriztion state during the transition. Two mass spectrometry (MS)-based protein analysis approaches were employed in this research (Figure 1). Here we

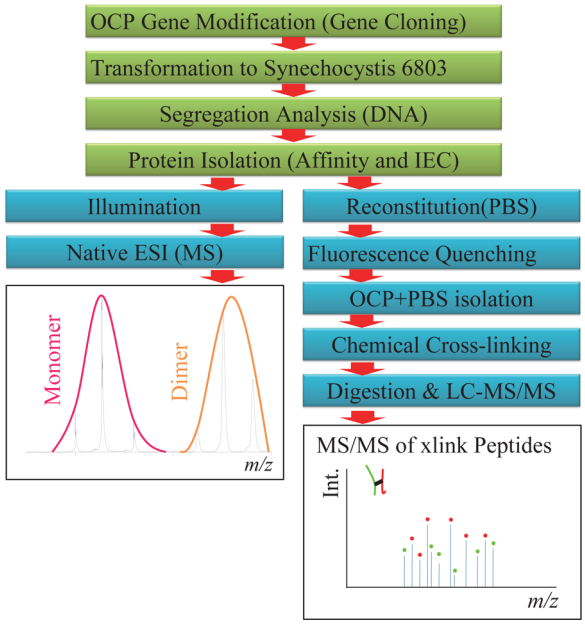

Figure 1. Schematic outline of the MS-based approach in studies of photoactivation and interaction of the OCP.

report the real time description of the OCP^o-to-OCP^r transition by using native MS, an emerging approach that allows for protein oligomerization-state analysis under nondenaturing conditions,[18,19] as well as for nonprotein cofactor stoichiometry analysis.[20] When combined with ion-mobility MS (IM-MS), this approach can be used to probe structural transitions of protein complexes in their near-native states.[21,22]

We are also interested in the structural location of the OCP^r in PBS, which still remains an open question[23,24] but is extremely important to the understanding of the molecular quenching mechanism from the point of view of the structural orientation of 3′-hECN and the chromophores in the PBS core. Site-directed mutagenesis suggested that R155 of the OCP in the N-terminal domain is involved in the stabilization of the OCP and in the interaction with PBS for fluorescence quenching.[13] Consensus has been reached that the OCP binds to the PBS core; however, the question of which APC (APC_{660} or APC_{680}) the OCP^r is binding is still controversial.[25,26] Both APC trimers have been suggested as the OCP binding site in previous publications from different groups.[23,25,27,28] Recently, MS-based protein cross-linking became a robust tool in the investigation of protein−protein interaction among large protein complexes.[29,30] In this study, a MS-based protein cross-linking experiment was also adopted to pinpoint the structural location of the OCP when it is bound to the PBS.

MATERIALS AND METHODS

Chemicals. Water, acetonitrile, formic acid, and ammonium acetate (all of LC grade) were purchased from Sigma-Aldrich (St. Louis, MO). Cross-linking reagents, bis(sulfosuccinimidyl) suberate (BS3), and disuccinimidyl suberate (DSS) were purchased from Pierce (Thermo Scientific). The HiTrap Q column was purchased from GE (Pittsburgh, PA).

Growth of *Synechocystis* sp. PCC 6803 and Mutant Construction. *Synechocystis* 6803 wild-type and C-terminally His_6-tagged OCP strain [OCP-His strain (see below)] were grown in BG11 medium[31] at 30 °C and a light intensity of 30 μmol of photons m^{-2} s^{-1} with supplementary antibiotic gentamicin (5 μg/mL). The fusion polymerase chain reaction (PCR) protocol[32] was used to construct a transformation cassette to replace the native OCP (*Slr1963*) in *Synechocystis* 6803 (Figure S1 of the Supporting Information). The OCP was purified as previously described[10] with minor modifications with a Bio-Rad fast performance liquid chromatography (FPLC) system. Briefly, to construct a transformation cassette, a partial *Slr1963* (OCP gene) sequence without the stop codon was amplified using the OCP1F (P1) and OCPGMR (P3) primers (Figure S1 and Table S1 of the Supporting Information). The PCR fragment contained the affinity tag (His_6), which was achieved from primer P3. The gentamicin cassette was amplified separately by PCR using primers P4 and P5. A fusion PCR product of partial *Slr1963* and gentamicin was produced and fused to the *Slr1963* downstream fragment. Segregation of the modified OCP was verified by PCR analysis using primer 2 and primer 5. The fully segregated strain was used for this study.

OCP and PBS Isolation. The HiTrap Q HP column [ion exchange chromatography (IEC)] was used for the cleanup after Ni-NTA affinity chromatography isolation. The isolated OCP was identified by sodium dodecyl sulfate−polyacrylamide gel electrophoresis and immunodetection (Figure S2 of the Supporting Information). The dark-adapted OCP was illuminated by white light at an intensity of ∼2000 μmol of photons m^{-2} s^{-1}. To prevent the buffer from being heated, the beam was first passed through an ∼10 cm water layer. Illumination resulted in rapid changes in the absorption spectra of the OCP as shown in Figure S3 of the Supporting Information.

Native MS of the OCP. The OCP sample was buffer exchanged with 200 mM ammonium acetate by using a 10 kDa molecular mass cutoff filter (Millipore Amicon Centrifugal Filters, Billerica, MA). Following buffer exchange, 10 μL (∼50 μM) was loaded onto an offline electrospray capillary (GlassTip 2 μm inside diameter, New Objective, Woburn, MA). The protein sample solution was injected into a hybrid ion mobility quadrupole time-of-flight mass spectrometer (Q-IM-TOF, SYNAPT G2 HDMS, Waters Inc., Milford, MA). The instrument was operated under gentle electrospray ionization (ESI) conditions (capillary voltage of 1.5−1.8 kV, sampling cone voltage of 20 V, extraction cone voltage of 2 V, and source temperature of 30 °C). The collision energy at the trap and transfer region was adjusted from 8 to 58 V for dissociating the OCP−3′-hECN complex. The pressure of the vacuum/backing region was 5.1−5.6 mbar. For the ion mobility measurements, the helium cell gas flow was 180 mL/min, the IMS gas flow was 90 mL/min, the IMS wave velocity was 650 m/s, and the IMS wave height was 40 V. Nitrogen was used as the mobility carrier gas. Each spectrum was acquired from m/z 1500 to 7500 every 1 s. The instrument was externally calibrated to m/z 8000 with

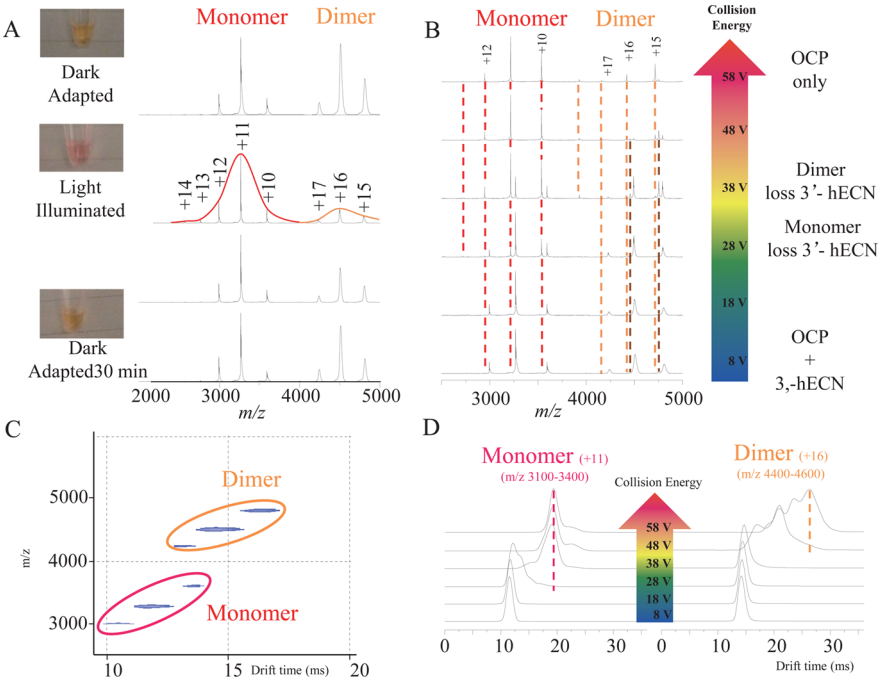

Figure 2. Native MS spectra of the OCP. (A) The dark-adapted (sample colored orange) OCP in 200 mM ammonium acetate was analyzed by native MS. Two charge envelopes were observed in the spectrum. The left envelope (labeled in red) corresponds to the MW of the monomeric OCP and one 3′-hECN. The right envelope (labeled in orange) corresponds to the MW of the dimeric OCP and two 3′-hECNs. The dark-adapted sample was illuminated with white light for 1.5 min. Two spectra were acquired when the OCP sample was restored to a dark environment for 5 and 30 min. (B) Native MS of the OCP with a collision energy ramp. (C) Two-dimensional IM-MS spectrum of the OCP sample. The *Y* axis shows the mass spectrometry measurement (mass to charge ratio, m/z), while the *X* axis shows the ion mobility measurement (drift time, milliseconds). Multiple charge states from two species were grouped into monomer (red) and dimer (orange). (D) Ion mobility measurement of the OCP. Two charge states, one for the OCP monomer (+11) and one for the OCP dimer (+16), were monitored by ion mobility with the collision energy ramp.

the clusters produced by ESI of a NaI solution. The peak picking and data processing were performed in Masslynx (version 4.1) and DriftScope (Waters Inc.).

PBS and OCP Reconstitution and Protein Cross-Linking Experiment. The PBS−OCP complexes were prepared in 0.8 M phosphate buffer (pH 7.0) by illumination of isolated PBS with 2000 μmol of photons of white light m^{-2} s^{-1} for 10 min at 23 °C in the presence of the OCP (OCP:PBS ratio of 40:1).[15] To separate the resulting PBS−OCP complexes from the unbound OCP after illumination, the sample was loaded onto a 100 kDa filter (Millipore Amicon Centrifugal Filters, Billerica, MA) and centrifuged at 4000*g* and 23 °C for 20 min. Fresh 0.8 M phosphate buffer was applied three times to dilute the retentate. The composition of the blue retentate was checked by absorption and fluorescence emission spectroscopies (Figure S4 of the Supporting Information). The concentration of PBS was calculated on the basis of the molar absorptivity formula.[15] The cross-linking experiment and LC−MS/MS were used as previously described with minor changes.[33] The PBS−OCP sample was resuspended at 0.1 μM based on the PB concentration calculation. BS3 and DSS cross-linking was performed according to the manufacturer's protocol followed by desalting using Zeba columns (Thermo Scientific, Waltham, MA) with minor modifications. Modified samples were precipitated using acetone, and the resuspended samples were directly subjected to trypsin digestion.

Trypsin Digestion and LC−MS Experiment. The digestion and LC−MS experimental protocol and data processing were adapted from previous publications. The details are given in the Supporting Information.

RESULTS AND DISCUSSION

Native MS Analysis of the Transition between the OCP^o and the OCP^r. Under standard ESI conditions, i.e., OCP in organic solvent, mass spectra show that the OCP is denatured, and the pigment (3′-hECN) is dissociated from the protein (Figure S5 of the Supporting Information). When the OCP^o was submitted to native ESI, however, it carries nearly 30 fewer charges than in the denatured conformation (Figure 2A and Figure S5 of the Supporting Information), suggesting retention of the near-native state. OCP samples with different concentrations (down to ∼10 μM) have been analyzed. Two charge-state distributions were observed. Two charge-state envelopes appear at relatively high m/z values (from m/z 2750 to 5000). Molecular weight (MW) assignment indicates that the low-m/z envelope (from 3000 to 3600) corresponds to an OCP monomer with one 3′-hECN (35.5 kDa, charge states from +10 to +12), whereas the high-m/z envelope (from 4200 to 5000) corresponds to the OCP dimer with two 3′-hECNs (71 kDa, charge states from +15 to +17). The overall abundances of the two states are similar with a monomer:dimer ratio of ∼1:1.

This observation presents the opportunity to use native MS to examine the monomer−dimer equilibrium as a function of light. When the dark-adapted OCP sample was illuminated by white light, the expected orange-to-red transition from the OCP^o to the active OCP^r was observed (Figure 2A and Figure S3 of the Supporting Information). The native mass spectrum, taken after illumination, shows a substantial loss of dimer; the monomer:dimer ratio became ∼5:1 (Figure 2A). Further, the charge-state distribution of the monomer OCP is extended

dx.doi.org/10.1021/bi401539w | *Biochemistry* 2014, 53, 13−19

higher (up to +14). We then stored the light-illuminated OCP sample in the dark to allow the reverse OCP^r-to-OCP^o transition to take place. After 5 min, the charge-state extension (up to +14) of the monomer disappeared, being replaced by a concomitant increase in the amount of dimer (monomer:dimer ratio of 5:2). When we analyzed the same OCP sample after 30 min in the dark, the monomer:dimer ratio had returned nearly to normal (~5:4), and the OCP sample had reassumed an orange color (Figure 2A).

The oligomeric state of the crystalline OCP is a dimer, as observed by X-ray crystallography.[8] There is no consensus, however, about the oligomeric state of the OCP in solution or *in vivo*. The relatively fast photochemical relaxation from the OCP^r to the OCP^o challenges traditional biochemistry approaches that monitor variations in stoichiometry such as biochemical preparation-based technology, like FPLC or HPLC. However, in our native MS, only 30 s elapsed between the sample light illumination and the collection of real time MS data. The entire MS running time for one sample is only 1−2 min. Our native MS experiment can also be used to reveal real time changes in the OCP oligomerization state that cannot be detected by denaturing, standard ESI (Figure S5 of the Supporting Information). Although the accurate quantitative information cannot be generated without an isotope-enriched internal standard, the conversion between the monomer and dimer can be obtained by native MS. The native MS results suggest that the monomeric form of the OCP becomes the dominant species in the light-illuminated OCP sample, whereas the dark-adapted OCP sample is a mixture of the monomer and dimer. Consistently, the dimeric oligomeric state of the OCP can be restored by keeping the light-illuminated OCP sample in the dark (Figure 2). The shift to a higher charge state upon illumination of the monomeric OCP is indicative of the presence of an "open" conformation of the OCP monomer. This open conformation may correspond to the OCP^r that interacts with the PBS.

Collision-Induced Dissociation of the OCP−Pigment Complex. We sought to characterize further the two oligomeric states found by native ESI of the dark-adapted OCP sample (OCP^o) (Figure 2B) by collisional activation of the gas-phase ions. When the collision energy of the mass spectrometer trap region was increased, the pigment dissociated from its protein binding site, allowing us to estimate the relative strengths of noncovalent carotenoid−OCP polypeptide interactions in both oligomeric states. The monomer shows only one mass shift peak that corresponds to the loss of a single 3′-hECN, while the dimer shows two mass shift peaks that correspond to the sequential loss of two 3′-hECNs. The 3′-hECNs are lost from the monomeric OCP at 28 V but at 38 V from the dimer. The majority of the OCP, both monomer and dimer, has lost 3′-hECN at 58 V. These results indicate that the OCP dimer binds 3′-hECN more tightly or 3′-hECN is more protected than in the OCP monomer and is more resistant to unfolding.

Ion Mobility Measurement of the OCP Monomer and Dimer. We also monitored the dissociation of 3′-hECN from the OCP with ion mobility (IM) upon introduction by native MS (Figure 2C,D). The OCP monomer and dimer, each containing three major charge states, can be separated by ion mobility. Comparing the drift time spectra of each oligomeric state, +11 for the monomer and +16 for the dimer, against the collision energy ramp, we found that single drift time distribution for each charge state at a low collision energy (8 V) became broader, split, and shifted to longer times, which was caused by protein conformational changes.[34] This result (Figure 2D) indicates that the cross section of the OCP for both monomer and dimer increased upon activation under the increased collision energy and adopted a more "unfolded" (larger size) conformational state. The drift time shift first occurred for the monomer at 38 V but occurred at 48 V for the dimer.

Previous studies have indicated that conformational changes of the OCP take place during the transition between the OCP^o and the OCP^r as monitored by amide I and amide II vibrational changes.[10] It was not known at that time whether transitions in the oligomerization state of the OCP are involved in this process. This is now resolved by native MS, which captures the interconversion between the monomeric and dimeric OCP. The CID and ion mobility experiments indicate that the pigment is more easily dissociated from the monomer than the dimer. The monomer has a more solvent-exposed 3′-hECN. The results from native MS and IM indicate that there is a light-induced conversion between the dimeric and monomeric OCP. Moreover, they suggest that this conversion is required in the transition of the OCP^o to the OCP^r and that the relatively open form of the monomer (with the extended charge state in native MS) is the active OCP^r.

Protein Cross-Linking of the PBS−OCP Complex. To locate the interface between the OCP and PBS, we used chemical cross-linking of lysine residues coupled with LC−MS/MS. We took advantage of a recent breakthrough that the PBS−OCP interaction can be reconstituted *in vitro*.[15] The OCP-mediated fluorescence quenching can also be observed from the *in vitro*-reconstituted PBS−OCP sample (Figure S4 of the Supporting Information). In our reconstitution experiments, changes in the 400−550 nm range of the absorption spectrum of the light-treated PBS−OCP mixture, taken before and after ultrafiltration, indicate effective removal of the unbound OCP (Figure S4A of the Supporting Information), underlying the stoichiometric binding of the OCP and PBS. PBS fluorescence further demonstrated that upon fast removal of the unbound OCP, the resulting PBS−OCP complex is still in a quenched state (Figure S4B of the Supporting Information), indicating that the OCP^r is bound to its functional site. This sample was immediately used for cross-linking reactions using bifunctional lysine specific reagents (see Materials and Methods). The cross-linked protein sample gave good sequence coverage of PBS components (ApcA, ApcB, ApcC, ApcE, ApcF, CpcA, CpcB, CpcC, CpcD, and CpcG) as well as of the OCP (Table S2 of the Supporting Information).

Protein cross-linking in combination with mass spectrometry has established a detailed catalog of product ion species.[29,35,36] In our experiments, 51 monolink peptides (attached to only one amino acid) were identified by LC−MS/MS (Figure S6 of the Supporting Information). There are 21 monolink peptides from the rod of PBS and 26 monolink peptides from the core of the PBS. Four monolink peptides were identified from the OCP. Loop-link peptides (where the cross-linker is attached to two amino acids within one peptide) were identified for both the PBS and the OCP. The most informative cross-linking species are cross-link peptides (where the cross-linker is attached to two different polypeptides), and 22 of these were identified. On the basis of those cross-link peptides (Figure S7 of the Supporting Information), we could map the interaction area between two protein fragments. The distance between two cross-linked sites can be elucidated with the consideration of

the flexibility of protein conformations. For example, the distance could be 9−24 Å with 11.4 Å cross-linkers, e.g., DSS BS3.[35] We also identified several intralink peptides (where the cross-linker is attached to two amino acids in the same polypeptide) within subunits. Because there are multiple copies for most of the PBS subunits in one PBS complex, the intralink peptides could be from one copy or two copies of the same subunit.

Given that the major goal of these experiments is to map the interaction between the OCP and PBS, we focused on the cross-link peptides between the OCP and PBS (Table S3 of the Supporting Information). Among the cross-link peptides, the lysine (K) cross-links are OCP K167−ApcB K58, OCP K249−ApcB K26, and OCP K170−ApcE K4 (Table S3 of the Supporting Information). All these lysines are solvent-exposed, according to the crystal structures of APC [Protein Data Bank (PDB) entry 4F0U] and the OCP (PDB entry 3MG1) from *Synechococcus elongatus* sp. PCC 7942 and *Synechocystis* sp. PCC 6803, respectively; the former protein sequence shares a high degree of identity with that of *Synechocystis* sp. PCC 6803.[8,17]

Although it is known that the photoactivated OCP^r protects the photosynthetic RCs by close interaction with the PBS and quenches the excess energy absorbed by PBS, the binding site remains elusive, and this greatly hampers the elucidation of the quenching mechanism. On the basis of our cross-linking experiments, we propose here a model of PBS−OCP interaction (Figure 3) by using model program i-TASSER.[37]

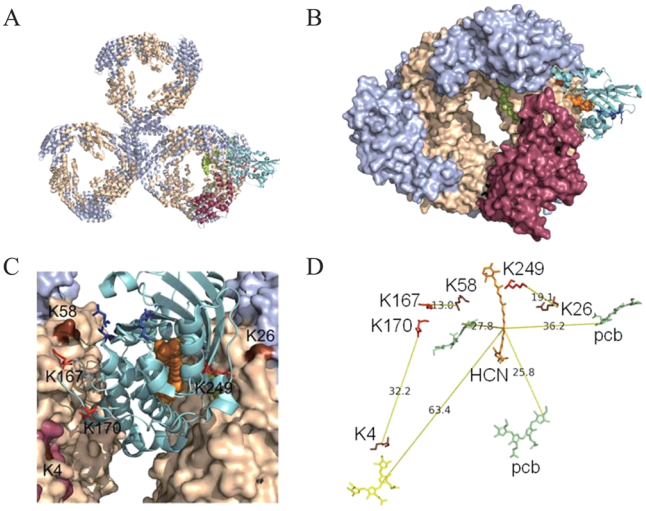

Figure 3. Structural location of the OCP in PBS. (A) The OCP (cyan) binds to the basal cylinder containing both APC_{660} trimers and APC_{680}: ApcA (light blue), ApcB (wheat), and ApcE (rasberry). The three-dimensional structure of the ApcE phycocyanobilin binding domain (raspberry) was predicted and was docked to one ApcA subunit.[38,39] (B) Close-up of the OCP between two basal APC trimers. The N-terminal domain of the OCP is buried within two APC trimers, leaving the C-terminal domain solvent-exposed, including D220, V232, and F299 (blue sticks). (C) View of the close association of the OCP with ApcB. Interlinks between ApcB K58 and OCP K167 and between ApcB K26 and OCP K249 are labeled, with sticks (K167 and K249 of the OCP) and surface (K58 and K26). The ApcE K4−OCP K170 interlink is rendered. 3′-hECN is presented as orange spheres. (D) Spatial relationships of 3′-hECN (HCN, orange sticks) and PCBs and lysine residues involved in cross-linking. D220, V232, and F299 are involved in the docking of fluorescence recovery protein (FRP, blue sticks): K4 (ApcE, brown sticks) and K26 and K58 (ApcB, brown sticks).

In this model, the OCP is located in the basal cylinder(s) of the PBS core instead of the upper one (Figure 3A,B). The N-terminal domain (residues 15−165)[8,17] is buried between two APC trimers, one APC_{660} and one APC_{680},[28] leaving the C-terminal domain solvent-accessible (Figure 3), with OCP K167 and OCP K249 located close to two adjacent ApcB proteins from APC_{680} and APC_{660} trimers, respectively. Our model suggests that there are only two OCP binding and, thus, quenching sites per PBS. These structural results based on LC−MS/MS spectra are in contrast to the hypothesis that the OCP can bind to any APC_{660}, which implies that there are more than two binding sites per PBS because of the multiple copies of APC_{660} in PBS.

The N- and C-terminal domains of the OCP are joined by a long (~25 amino acids) peptide chain. Even though this is the only region of the protein that is not strongly conserved, we found that K167 and K170 in this linker are cross-linked to ApcB K58 and ApcE K4, respectively (Table S3 of the Supporting Information). It seems that this flexible linker could pass conformational information from the C-terminal domain to the buried N-terminal domains of the protein or vice versa and thereby allow the energy coupling of 3′-hECN and phycocyanobilins (PCBs). According to our model, PCB pigments from APC_{660} are located spatially closer to the pigment of the OCP than PCB is to ApcE. Because spatial distance dictates the excitation energy transfer efficiency, we hypothesize that the OCP^r will preferentially quench the excitation energy from APC_{660}. Similar conclusions about quenching sites were recently proposed on the basis of spectroscopic methods and mutation studies.[26,27,40] We think that our results constitute direct structural evidence that supports this hypothesis. There are reports showing that ApcE (L_{CM}) could also be the binding partner of the OCP and that ApcE is directly involved in the OCP-mediated NPQ.[23,25] Our data do not exclude this hypothesis; however, if this were the case, the quenching efficiency would be very low *in vivo*, because of the increased spatial distance between 3′-hECN and the terminal emitter on ApcE (Figure 3). Additionally, nonphysiological conditions (2 M urea at pH 2.5 or 60 mM formic acid at pH 3.0) used in the preparation of ApcE and in the reconstitution of the ApcE−OCP complex in these two reports could lead to unexpected results.[4]

It was proposed previously that the N-terminal domain of the OCP that contains R155 is directly involved in the binding of the OCP^r to APC trimers based on site-directed mutagenesis and quenching analysis. Furthermore, breakage of the R155−E244 salt bridge could play an important role during the activation of the OCP.[13] There are multiple APC trimers, including multiple APC_{660} species and at least two APC_{680} species, in the PBS core. Determining which APC trimer the OCP^r is binding will improve our understanding of the detailed photoprotection mechanism in cyanobacteria. Our results narrow down the OCP binding site to the cleft formed between two APC trimers and thus will facilitate future experiments such as determining which amino acids on either the OCP or the ApcB are playing important roles in the stabilization or destabilization of the quenching complex.

The C-terminal domain of the OCP (D220, V232, and F299) was recently shown to be involved in the interactions between FRP,[16] which *in vivo* is essential to recovering the full capacity of the PBS light harvesting function, presumably by playing a role in detaching the OCP^r. In our model, three amino acid residues (D220, V232, and F299) are located on the

dx.doi.org/10.1021/bi401539w | *Biochemistry* 2014, 53, 13−19

C-terminal domain of the OCP, consistent with the docking and co-immunoprecipitation analysis.[16]

CONCLUSIONS

Evidence from native MS that the transient conversion of the OCP^o to the OCP^r involves the monomerization of the OCP, which is competent to bind to the PBS for fluorescence quenching and photoprotection, is presented here. Protein cross-linking analysis further indicates that the N-terminal domain of the OCP is buried between the APC_{660} trimer and the APC_{680} trimer in the PBS core. This structural information about the OCP provides a basis for future studies of the detailed interactions between the 3′-hECN and chromophores in the PBS core and the regulation of light harvesting.

The potential of MS-based approaches in studies of OCP-related photoactivation has been demonstrated. Although MS-based approaches cannot provide high-resolution structural information, the speed and sensitivity of MS will further benefit the investigation of OCP-related photoactivation in cyanobacteria.

ASSOCIATED CONTENT

Supporting Information

Experimental procedures and additional data. This material is available free of charge via the Internet at http://pubs.acs.org.

AUTHOR INFORMATION

Corresponding Author

*Departments of Biology and Chemistry, Washington University in St. Louis, CB1137, One Brookings Dr., St. Louis, MO 63130. E-mail: blankenship@wustl.edu. Fax: (314) 935-4432. Telephone: (314) 935-7971.

Funding

This research was supported by the Photosynthetic Antenna Research Center, an Energy Frontier Research Center funded by the U.S. Department of Energy (DOE), Office of Basic Energy Sciences (Grant DE-SC 0001035 to R.E.B.), and National Institute of General Medical Sciences (NIGMS) (Grant 8 P41 GM103422-35 to M.L.G.). H.L., D.M.N., M.P., and J.J. were funded by the DOE grant; H.Z. was funded equally by the DOE and NIGMS grants, and instrumentation was made available by both the DOE- and NIGMS-supported programs.

Notes

The authors declare no competing financial interest.

REFERENCES

(1) Glazer, A. N. (1988) Phycobiliproteins. *Methods Enzymol. 167*, 291−303.

(2) Peschek, G. (1999) Photosynthesis and Respiration of Cyanobacteria. In *The Phototrophic Prokaryotes* (Peschek, G., Löffelhardt, W., and Schmetterer, G., Eds.) pp 201−209, Springer, New York.

(3) Niyogi, K. K., and Truong, T. B. (2013) Evolution of flexible non-photochemical quenching mechanisms that regulate light harvesting in oxygenic photosynthesis. *Curr. Opin. Plant Biol. 16*, 307−314.

(4) Kirilovsky, D., and Kerfeld, C. A. (2013) The Orange Carotenoid Protein: A blue-green light photoactive protein. *Photochem. Photobiol. Sci. 12*, 1135−1143.

(5) Kirilovsky, D., and Kerfeld, C. A. (2012) The orange carotenoid protein in photoprotection of photosystem II in cyanobacteria. *Biochim. Biophys. Acta 1817*, 158−166.

(6) Holt, T. K., and Krogmann, D. W. (1981) A carotenoid-protein from cyanobacteria. *Biochim. Biophys. Acta 637*, 408−414.

(7) Wu, Y. P., and Krogmann, D. W. (1997) The orange carotenoid protein of *Synechocystis* PCC 6803. *Biochim. Biophys. Acta 1322*, 1−7.

(8) Kerfeld, C. A., Sawaya, M. R., Brahmandam, V., Cascio, D., Ho, K. K., Trevithick-Sutton, C. C., Krogmann, D. W., and Yeates, T. O. (2003) The crystal structure of a cyanobacterial water-soluble carotenoid binding protein. *Structure 11*, 55−65.

(9) Wilson, A., Ajlani, G., Verbavatz, J. M., Vass, I., Kerfeld, C. A., and Kirilovsky, D. (2006) A soluble carotenoid protein involved in phycobilisome-related energy dissipation in cyanobacteria. *Plant Cell 18*, 992−1007.

(10) Wilson, A., Punginelli, C., Gall, A., Bonetti, C., Alexandre, M., Routaboul, J. M., Kerfeld, C. A., van Grondelle, R., Robert, B., Kennis, J. T., and Kirilovsky, D. (2008) A photoactive carotenoid protein acting as light intensity sensor. *Proc. Natl. Acad. Sci. U.S.A. 105*, 12075−12080.

(11) Polivka, T., Chabera, P., and Kerfeld, C. A. (2013) Carotenoid-protein interaction alters the S(1) energy of hydroxyechinenone in the Orange Carotenoid Protein. *Biochim. Biophys. Acta 1827*, 248−254.

(12) Berera, R., van Stokkum, I. H., Gwizdala, M., Wilson, A., Kirilovsky, D., and van Grondelle, R. (2012) The photophysics of the orange carotenoid protein, a light-powered molecular switch. *J. Phys. Chem. B 116*, 2568−2574.

(13) Wilson, A., Gwizdala, M., Mezzetti, A., Alexandre, M., Kerfeld, C. A., and Kirilovsky, D. (2012) The essential role of the N-terminal domain of the orange carotenoid protein in cyanobacterial photoprotection: Importance of a positive charge for phycobilisome binding. *Plant Cell 24*, 1972−1983.

(14) Stadnichuk, I. N., Yanyushin, M. F., Zharmukhamedov, S. K., Maksimov, E. G., Muronets, E. M., and Pashchenko, V. Z. (2011) Quenching of phycobilisome fluorescence by orange carotenoid protein. *Dokl. Biochem. Biophys. 439*, 167−170.

(15) Gwizdala, M., Wilson, A., and Kirilovsky, D. (2011) In vitro reconstitution of the cyanobacterial photoprotective mechanism mediated by the Orange Carotenoid Protein in *Synechocystis* PCC 6803. *Plant Cell 23*, 2631−2643.

(16) Sutter, M., Wilson, A., Leverenz, R. L., Lopez-Igual, R., Thurotte, A., Salmeen, A. E., Kirilovsky, D., and Kerfeld, C. A. (2013) Crystal structure of the FRP and identification of the active site for modulation of OCP-mediated photoprotection in cyanobacteria. *Proc. Natl. Acad. Sci. U.S.A. 110*, 10022−10027.

(17) Wilson, A., Kinney, J. N., Zwart, P. H., Punginelli, C., D'Haene, S., Perreau, F., Klein, M. G., Kirilovsky, D., and Kerfeld, C. A. (2010) Structural Determinants Underlying Photoprotection in the Photoactive Orange Carotenoid Protein of Cyanobacteria. *J. Biol. Chem. 285*, 18364−18375.

(18) Benesch, J. L., Ruotolo, B. T., Simmons, D. A., and Robinson, C. V. (2007) Protein complexes in the gas phase: Technology for structural genomics and proteomics. *Chem. Rev. 107*, 3544−3567.

(19) Heck, A. J. R., and van den Heuvel, R. H. H. (2004) Investigation of intact protein complexes by mass spectrometry. *Mass Spectrom. Rev. 23*, 368−389.

(20) Zhang, H., Cui, W., Gross, M. L., and Blankenship, R. E. (2013) Native mass spectrometry of photosynthetic pigment−protein complexes. *FEBS Lett. 587*, 1012−1020.

(21) Zhong, Y., Hyung, S. J., and Ruotolo, B. T. (2012) Ion mobility-mass spectrometry for structural proteomics. *Expert Rev. Proteomics 9*, 47−58.

(22) Uetrecht, C., Rose, R. J., van Duijn, E., Lorenzen, K., and Heck, A. J. R. (2010) Ion mobility mass spectrometry of proteins and protein assemblies. *Chem. Soc. Rev. 39*, 1633−1655.

(23) Stadnichuk, I. N., Yanyushin, M. F., Maksimov, E. G., Lukashev, E. P., Zharmukhamedov, S. K., Elanskaya, I. V., and Paschenko, V. Z. (2012) Site of non-photochemical quenching of the phycobilisome by orange carotenoid protein in the cyanobacterium *Synechocystis* sp. PCC 6803. *Biochim. Biophys. Acta 1817*, 1436−1445.

(24) Kuzminov, F. I., Karapetyan, N. V., Rakhimberdieva, M. G., Elanskaya, I. V., Gorbunov, M. Y., and Fadeev, V. V. (2012) Investigation of OCP-triggered dissipation of excitation energy in PSI/

PSII-less *Synechocystis* sp. PCC 6803 mutant using non-linear laser fluorimetry. *Biochim. Biophys. Acta 1817*, 1012−1021.
(25) Stadnichuk, I. N., Yanyushin, M. F., Bernat, G., Zlenko, D. V., Krasilnikov, P. M., Lukashev, E. P., Maksimov, E. G., and Paschenko, V. Z. (2013) Fluorescence quenching of the phycobilisome terminal emitter L from the cyanobacterium *Synechocystis* sp. PCC 6803 detected in vivo and in vitro. *J. Photochem. Photobiol., B 125C*, 137−145.
(26) Jallet, D., Gwizdala, M., and Kirilovsky, D. (2012) ApcD, ApcF and ApcE are not required for the Orange Carotenoid Protein related phycobilisome fluorescence quenching in the cyanobacterium *Synechocystis* PCC 6803. *Biochim. Biophys. Acta 1817*, 1418−1427.
(27) Tian, L. J., Gwizdala, M., van Stokkum, I. H. M., Koehorst, R. B. M., Kirilovsky, D., and van Amerongen, H. (2012) Picosecond Kinetics of Light Harvesting and Photoprotective Quenching in Wild-Type and Mutant Phycobilisomes Isolated from the Cyanobacterium *Synechocystis* PCC 6803. *Biophys. J. 102*, 1692−1700.
(28) Jallet, D., Gwizdala, M., and Kirilovsky, D. (2012) ApcD, ApcF and ApcE are not required for the Orange Carotenoid Protein related phycobilisome fluorescence quenching in the cyanobacterium *Synechocystis* PCC 6803. *Biochim. Biophys. Acta 1817*, 1418−1427.
(29) Sinz, A. (2006) Chemical cross-linking and mass spectrometry to map three-dimensional protein structures and protein-protein interactions. *Mass Spectrom. Rev. 25*, 663−682.
(30) Petrotchenko, E. V., and Borchers, C. H. (2010) Crosslinking combined with mass spectrometry for structural proteomics. *Mass Spectrom. Rev. 29*, 862−876.
(31) Allen, M. M., and Stanier, R. Y. (1968) Growth and division of some unicellular blue-green algae. *J. Gen. Microbiol. 51*, 199−202.
(32) Szewczyk, E., Nayak, T., Oakley, C. E., Edgerton, H., Xiong, Y., Taheri-Talesh, N., Osmani, S. A., and Oakley, B. R. (2006) Fusion PCR and gene targeting in *Aspergillus nidulans*. *Nat. Protoc. 1*, 3111−3120.
(33) Herzog, F., Kahraman, A., Boehringer, D., Mak, R., Bracher, A., Walzthoeni, T., Leitner, A., Beck, M., Hartl, F. U., Ban, N., Malmstrom, L., and Aebersold, R. (2012) Structural probing of a protein phosphatase 2A network by chemical cross-linking and mass spectrometry. *Science 337*, 1348−1352.
(34) Politis, A., Park, A. Y., Hyung, S. J., Barsky, D., Ruotolo, B. T., and Robinson, C. V. (2010) Integrating ion mobility mass spectrometry with molecular modelling to determine the architecture of multiprotein complexes. *PLoS One 5*, e12080.
(35) Leitner, A., Walzthoeni, T., Kahraman, A., Herzog, F., Rinner, O., Beck, M., and Aebersold, R. (2010) Probing native protein structures by chemical cross-linking, mass spectrometry, and bioinformatics. *Mol. Cell. Proteomics 9*, 1634−1649.
(36) Bruce, J. E. (2012) In vivo protein complex topologies: Sights through a cross-linking lens. *Proteomics 12*, 1565−1575.
(37) Roy, A., Kucukural, A., and Zhang, Y. (2010) I-TASSER: A unified platform for automated protein structure and function prediction. *Nat. Protoc. 5*, 725−738.
(38) Zhang, Y. (2008) I-TASSER server for protein 3D structure prediction. *BMC Bioinf. 9*, 40.
(39) Liu, H., Zhang, H., Niedzwiedzki, D. M., Prado, M., He, G., Gross, M. L., and Blankenship, R. E. (2013) Phycobilisomes supply excitations to both photosystems in a megacomplex in cyanobacteria. *Science 342*, 1104−1107.
(40) Tian, L., van Stokkum, I. H., Koehorst, R. B., Jongerius, A., Kirilovsky, D., and van Amerongen, H. (2011) Site, rate, and mechanism of photoprotective quenching in cyanobacteria. *J. Am. Chem. Soc. 133*, 18304−18311.